REPORT SD-TR-89-49

Spin–Orbit Relaxation Rates of $Bi(6p^3\ ^2D_{3/2})$ Following Photolysis of $Bi(CH_3)_3$ at $\lambda = 193$ nm

J. S. HOLLOWAY, J. B. KOFFEND, and R. F. HEIDNER, III
Aerophysics Laboratory
Laboratory Operations
The Aerospace Corporation
El Segundo, CA 90245

7 July 1989

Prepared for

WEAPONS LABORATORY
Kirtland Air Force Base, N. M. 87117

SPACE SYSTEMS DIVISION
AIR FORCE SYSTEMS COMMAND
Los Angeles Air Force Base
P.O. Box 92960
Los Angeles, CA 90009-2960

This report was submitted by The Aerospace Corporation, El Segundo, CA 90245, under Contract No. F04701-88-C-0089 with the Space Systems Division, P. O. Box 92960, Los Angeles, CA 90009. It was reviewed and approved for The Aerospace Corporation by W. P. Thompson, Director, Aerophysics Laboratory. Capt Scott W. Levinson was the Air Force project officer.

This report has been reviewed by the Public Affairs Office (PAS) and is releasable to the National Technical Information Service (NTIS). At NTIS, it will be available to the general public, including foreign nationals.

This technical report has been reviewed and is approved for publication. Publication of this report does not constitute Air Force approval of the report's findings or conclusions. It is published only for the exchange and stimulation of ideas.

SCOTT V. LEVINSON, CAPT, USAF
MOIE Project Officer
SSD/CNID

JAMES A. BERES, LT COL, USAF
MOIE Program Manager
AFSTC/WCO OL-AB

UNCLASSIFIED

SECURITY CLASSIFICATION OF THIS PAGE

REPORT DOCUMENTATION PAGE

1a. REPORT SECURITY CLASSIFICATION Unclassified	1b. RESTRICTIVE MARKINGS
2a. SECURITY CLASSIFICATION AUTHORITY	3. DISTRIBUTION/AVAILABILITY OF REPORT Approved for public release; distribution unlimited
2b. DECLASSIFICATION/DOWNGRADING SCHEDULE	
4. PERFORMING ORGANIZATION REPORT NUMBER(S) TR-0089(4604)-1	5. MONITORING ORGANIZATION REPORT NUMBER(S) SD-TR-89-49
6a. NAME OF PERFORMING ORGANIZATION The Aerospace Corporation Laboratory Operations 6b. OFFICE SYMBOL (If applicable)	7a. NAME OF MONITORING ORGANIZATION Space Systems Division
6c. ADDRESS (City, State, and ZIP Code) El Segundo, CA 90245	7b. ADDRESS (City, State, and ZIP Code) Los Angeles Air Force Base Los Angeles, CA 90009-2960
8a. NAME OF FUNDING/SPONSORING ORGANIZATION Weapons Laboratory 8b. OFFICE SYMBOL (If applicable)	9. PROCUREMENT INSTRUMENT IDENTIFICATION NUMBER F04701-88-C-0089
8c. ADDRESS (City, State, and ZIP Code) Kirtland Air Force Base, NM 87117	10. SOURCE OF FUNDING NUMBERS PROGRAM ELEMENT NO. / PROJECT NO. / TASK NO. / WORK UNIT ACCESSION NO.

11. TITLE (Include Security Classification)
Spin-Orbit Relaxation Rates of Bi($6p^3\ ^2D_{3/2}$) Following Photolysis of $Bi(CH_3)_3$ at λ = 193 nm

12. PERSONAL AUTHOR(S)
Holloway, J. S., Koffend, J. B.; and Heidner, R. F.

13a. TYPE OF REPORT	13b. TIME COVERED	14. DATE OF REPORT (Year, Month, Day)	15. PAGE COUNT
	FROM _____ TO _____	1989 July 7	28

16. SUPPLEMENTARY NOTATION

17. COSATI CODES		
FIELD	GROUP	SUB-GROUP

18. SUBJECT TERMS (Continue on reverse if necessary and identify by block number)
Interaction modeling
Excimer laser
Isotopic substitution

19. ABSTRACT (Continue on reverse if necessary and identify by block number)

Rate coefficients for the collisional relaxation of the first excited spin-orbit state of Bi ($6p^3$, $^2D_{3/2}$) have been measured at 295 K for Ar, CO_2, SF_6, H_2, D_2, HF, and DF. The excited Bi atoms were prepared by excimer laser photolysis of trimethyl bismuth (TMB) at 193 nm and monitored directly in emission. The rate coefficient for quenching by the precursor TMB and a lower limit for removal by CH_3 photofragments have also been established. Where applicable, our results are compared with the earlier work of Bevan and Husain and of Trainor. The suitability of long-range interaction models is discussed for those cases where isotopic substitution leads to markedly different quenching rates.

20. DISTRIBUTION/AVAILABILITY OF ABSTRACT	21. ABSTRACT SECURITY CLASSIFICATION
☒ UNCLASSIFIED/UNLIMITED ☐ SAME AS RPT. ☐ DTIC USERS	Unclassified
22a. NAME OF RESPONSIBLE INDIVIDUAL	22b. TELEPHONE (Include Area Code) / 22c. OFFICE SYMBOL

DD FORM 1473, 84 MAR

83 APR edition may be used until exhausted.
All other editions are obsolete

SECURITY CLASSIFICATION OF THIS PAGE
UNCLASSIFIED

PREFACE

We wish to express our gratitude to the Weapons Laboratory and Capt. Glen Perram for their continuing support of this research. We also extend our thanks to J. F. Bott for his help with the methyl radicals kinetics and to J. M. Herbelin for insight into the NF/BiF system.

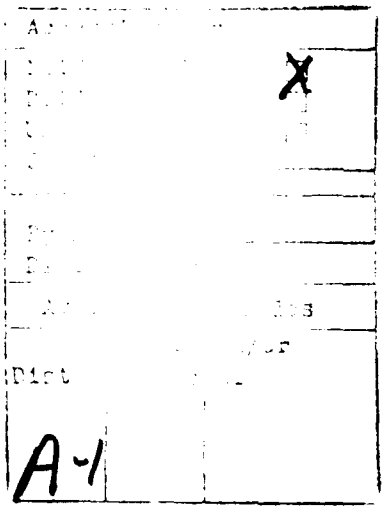

CONTENTS

FIGURES

TABLES

I. INTRODUCTION

The collisional behavior of the first two excited spin-orbit states of the bismuth $6p^3$ ground state configuration ($^2D_{3/2,5/2}$) has been the subject of a number of investigations.[1-4] Because they share the same electronic configuration as the $^4S_{3/2}$ ground state, these states are optically metastable. As such they provide a convenient venue for the study of collisional relaxation of electronically excited atoms. In turn, the results of these experiments have been useful in understanding heavy atom-molecule collisions and the strengths and limitations of employing (J,Ω) coupling approximations in treating them. Quenching studies of low-lying spin-orbit states have also provided direct evidence of electronic to vibrational $(E \rightarrow V)$ energy transfer.[5]

The development of electronic transition lasers has also required an increased understanding of the kinetics of metastable atoms. As an example, the 472 nm pulsed Bi vapor laser terminates on the $^2D_{3/2}$ level. Knowledge of that state's relaxation and removal processes is critical to evaluation of the device's performance.

Our laboratory's interest in low-lying Bi metastables dates from the discovery of the efficient, near-resonant electronic energy transfer between the first excited state of nitrogen fluoride and the ground-state of Bi[6]

$$NF(a^1\Delta) + Bi(^4S_{3/2}) \rightarrow NF(X^3\Sigma) + Bi(^2D_{3/2});\ \Delta E = -16\ cm^{-1} \qquad (1)$$

Reanalysis of this experiment, in light of the subsequently reported lifetime of $NF(a^1\Delta)$ of 5.6 sec,[7] gives a rate constant $k_1 = 1.8 \times 10^{-10}$ cm^3/molec-sec. It has been postulated that $Bi(^2D_{3/2})$ can further react with another $NF(a^1\Delta)$ molecule to produce electronically excited BiF[8]

$$NF(a^1\Delta) + Bi(^2D_{3/2}) \rightarrow BiF(A0^+,v) + N(^4S_{3/2}) \qquad (2)$$

Evidence suggests that this reaction is both fast (ca. 8×10^{-11} cm^3/molec-sec) and selective, creating the potential for a population inversion on the $BiF(A0^+ \rightarrow X0^+)$ transition in the 430-480 nm spectral region. Employing densities of $NF(a^1\Delta)$ on the order of 10^{10} cm^{-3}, virtually complete inversions of $Bi(^2D_{3/2})$ have been achieved at the 10^8 cm^{-3} number density level.[9] In experiments scaled to higher densities ($[NF(a^1\Delta)] \approx 10^{13}$ $[Bi] \approx 10^{10}$ cm^{-3}), it was found that a substantial fraction of the available Bi was converted to BiF, with strong emission observed from the blue $BiF(A \rightarrow X)$ band system.[10]

$NF(a^1\Delta)$ is conveniently produced by means of the H_2/NF_2 chain reaction[11]

$$F + H_2 \rightarrow HF(v) + H \tag{3}$$

$$H + NF_2 \rightarrow NF(a^1\Delta) + F \tag{4}$$

in which reaction 4 produces the $(a^1\Delta)$ state with a branching ratio of >0.9.[7,12] Thus, we have a system capable of producing a reservoir of chemical energy in extremely high yield (reactions 3 and 4) which may be coupled to an efficient mechanism (reactions 1 and 2) for extracting that energy in the form of an electronically excited diatomic molecule with a radiative transition in the blue region of the visible spectrum. The system described is a promising visible chemical laser candidate.[13]

The purpose of the present study is to investigate those removal processes of $Bi(^2D_{3/2})$ that pertain to the chemical milieu of the laser system. The current investigation has been limited to those cases in which nonreactive collisions are expected to be the dominant removal mechanism. The species of interest include $H_2(D_2)$ and HF(DF). A frequently employed photolytic source of Bi is trimethyl bismuth (TMB), $(Bi(CH_3)_3$. The rate coefficient for TMB has been determined, as well as a lower limit for quenching by daughter CH_3 fragments. Additionally, rate coefficients for the inert gases Ar, SF_6, and CO_2 have been obtained.

II. EXPERIMENTAL APPARATUS AND PROCEDURE

In approaching this study we have tried not only to extend the available body of knowledge on the subject, but also to improve upon the methodology of previous work. Earlier kinetics studies have relied on flash photolysis of TMB to generate the excited Bi atom population[2-4], and resonant atomic absorption to monitor the ^2D states. The broadband ultraviolet output of the flashlamps was found to lead to the formation of a remarkably large number of species,[1] while the relatively long duration of the pulse imposed a substantial lower limit on the temporal resolution of the experiments. Because the atomic states were monitored in absorption, the signal-to-noise ratio of those studies was determined by the characteristics of the line sources used.[2,3] An additional complication encountered in the use of an absorption probe is the necessity of determining the experimental parameter γ in the modified Beer-Lambert expression[14]

$$I = I_o \exp(-\varepsilon(cl)^{\gamma})$$

where the symbols have their usual meaning. We have departed from past work in two significant respects. We have chosen ArF excimer laser photolysis of TMB at 193 nm to create our initial $Bi(^2D_{3/2})$ population. By so doing we are able to deposit the photolysis energy into the parent species in a relatively well-characterized manner. This approach also makes it much easier to discriminate against scattered light in our optical detection channel, thereby affording the experiment a time resolution limited in principle only by the 14 nsec excimer pulse. Secondly, we can observe $Bi(^2D_{3/2})$ directly in emission at 876 nm via a narrowband interference filter and a red sensitive GaAs photomultiplier tube. As a result, we have extremely sensitive detection and simplified data analysis in comparison to earlier work.

Our experimental layout, depicted schematically in Fig. 1, consists of a temperature-controlled flow reactor and associated gas-handling manifold, an excimer photolysis laser, and signal detection and acquisition instrumentation. The flow cell is of stainless steel construction, 25 cm in length by 4.6 cm i.d., internally coated with Teflon to reduce the rate of radical recombination at the walls. Three viewing ports are located at right angles to the flow axis, which is also the photolysis axis. Aluminum extension pieces, 15 cm in length, have been added to both ends of the cell. These allow for the addition of a purge on the entrance window plus a stack of light baffles and a Brewster's angle mount on the exit window. The purge is necessary to prevent the transmission of the window from degrading due to the accumulation of bismuth metal after a number of photolysis pulses. The baffles and Brewster's window are used to reduce scattered excimer light. Suprasil windows are used on all cell ports for most of the experiments. These were replaced with CaF_2 windows on the observation ports and MgF_2 windows on the excimer photolysis ports for the quenching measurements with HF and DF.

Reagent gases were premixed and introduced in the central stainless steel/Teflon section of the cell. Flow rates were measured with mass flow meters (Tylan) which had been calibrated in situ. Pressure was measured by a capacitance manometer (MKS) with 10 mTorr resolution. Total flow rates were typically less than 1.0 l-atm/min. Overall cell pressure (on the order of 30-80 Torr) and the partial pressure of TMB (about 1×10^{-4} torr for most runs) were held constant with Ar as the buffer gas for each set of measurements so that system heat capacity, diffusion, and $Bi(^2D_{3/2})$ removal by Ar and TMB would in turn be constant factors in each determination.

An excimer laser (Lambda Physik EMG 101) was operated with ArF at 193 nm to produce the 14 nsec photolysis pulse. Because of the marked power dependence of the $Bi(^2D_{3/2})$ decay rate, we chose to attenuate the excimer output by means of a stack of fused silica flats to a level that resulted in reasonably long baseline decay times without sacrificing signal to noise. Photolysis fluences on the order of 5-10 mJ/cm^2 were typically

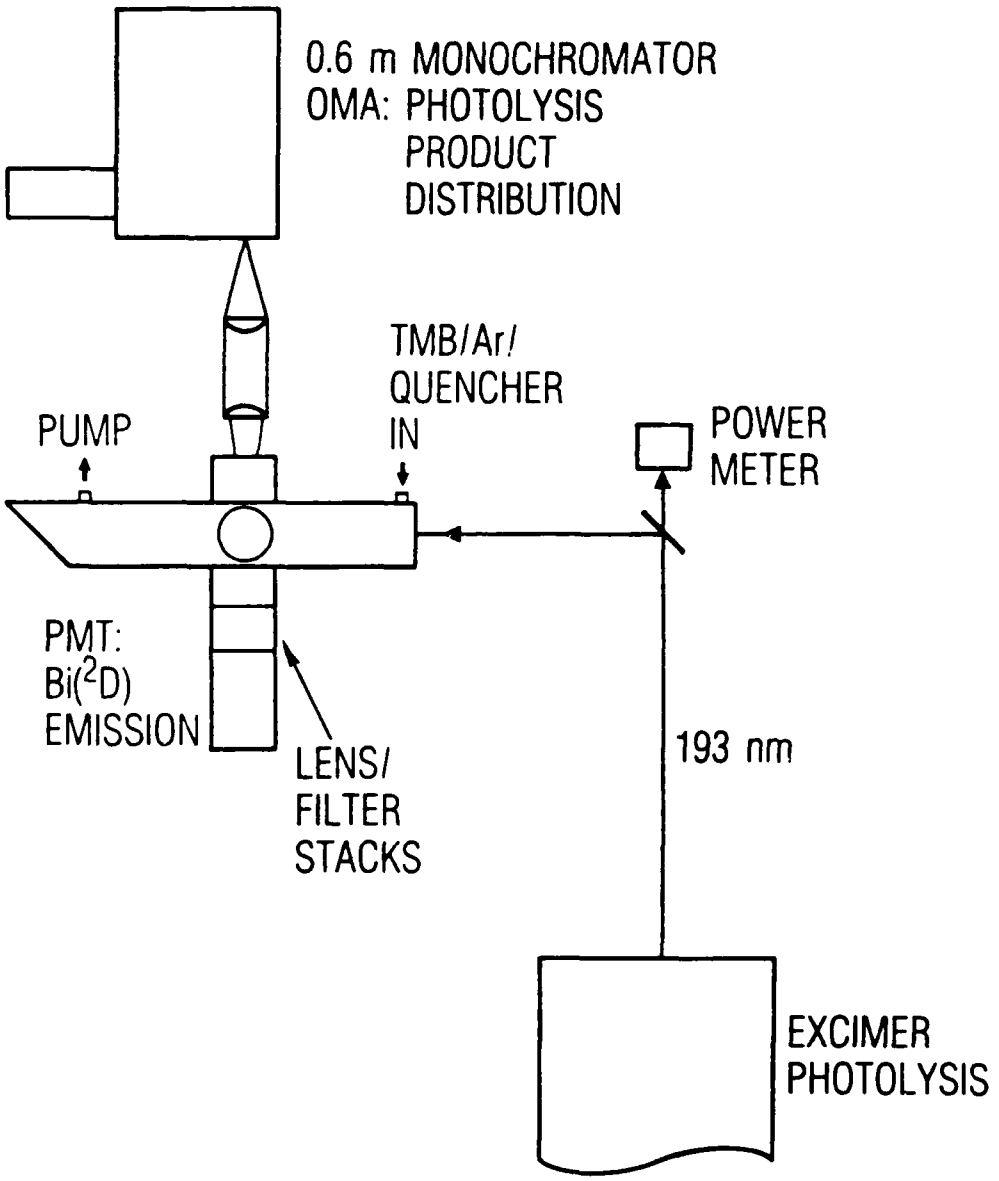

Fig. 1. Block Diagram of Experimental Arrangement.

used, although fluences as high as 60 mJ/cm^2 were employed for power dependence measurements. Energy was determined using a cavity type joulemeter (Laser Precision) to sample the fraction of 193 nm radiation transmitted by the excimer-turning mirror and calibrated against a thermal power meter (Coherent) positioned directly in front of the entrance window of the cell. The experiments were conducted at repetition rates of 2.0 to 0.5 Hz to assure the removal of photolysis products between pulses.

Our diagnostics consist of a thermoelectrically cooled GaAs phototube (RCA C31034) which collects $Bi(^2D_{3/2})$ emission through a narrow-band interference filter (876.0 nm, 0.64 nm FWHM) following the photolysis of TMB. The signal is amplified (Tektronix 502) and collected with a transient digitizer (LeCroy 2264) and averaged with a laboratory computer (DEC LSI 11/73). Total photolysis emission is resolved with a 0.6 m monochromator (McPherson 207) and recorded with an optical multichannel analyzer (OMA; EG&G PARC 1461 with 1420BR intensified diode array).

A 0.1% mixure of TMB (ICN Pharmaceuticals) in Ar was used. Hydrogen fluoride and deuterium fluoride samples (Matheson) were purified by several freeze-pump-thaw cycles in a stainless steel vessel. The HF and DF were run as 20% mixtures diluted with Ar. The other reagents were: Ar (Matheson UHP; 99.999%), CO_2 (Alphagaz Research Grade; 99.998%), H_2 (Matheson UHP; 99.999%), D_2 (98%), and SF_6 (Matheson Instrument Purity; 99.99%).

III. RESULTS AND DISCUSSION

We observe (in emission) a wide disposition in the energy of the Bi resulting from ArF laser photolysis of TMB. In OMA traces from 2200 to 6500 Å we can unambiguously identify 16 lines,[15] which originate from 11 excited states of Bi with energies of up to almost 50000 cm^{-1}. We also observe a blue-degraded band structure at about 4315 Å, which is probably attributable to Bi_2.

Of the 11 excited states lying above $Bi(^2D_{3/2})$ that we observe, all but the three other excited spin-orbit states of the $6p^3$ ground state configuration ($^2P_{3/2,1/2}$ and $^2D_{5/2}$) possess dipole-allowed transitions to either $^4S°$ or $^2D_{3/2}$. These states can reasonably be expected to be short lived. Of the other $6p^3$ states, only $^2D_{5/2}$ has a longer radiative lifetime ($A = 12.4\ sec^{-1}$)[16] than the $^2D_{3/2}$ state. Both Bevan and Husain[2] and Trainor[3] found that the J = 5/2 state was removed more rapidly with all collision partners studied than was the J = 3/2 state. Therefore, all positive contributions, via either radiative transitions or collisional cascading, to the $^2D_{3/2}$ population should take place on a time scale that is short in relation to the exponentially decaying portion of the data on which the removal rates are based.

Our technique for determining decay rates of the $Bi(^2D_{3/2})$ state is straightforward. Following the photolysis pulse, we observe an emission signal that rises from some instantaneous value with a time constant on the order of $0.1\text{-}30 \times 10^5\ sec^{-1}$ (depending on conditions), followed by a slower decay. Such traces can be fit well by a rising plus a falling exponential. Figure 2 provides an example of two representitive time histories and their associated fits for $Bi(^2D_{3/2})$ with and without H_2 in 40 torr of Ar. The rate of decay we measure is the sum of the rates of diffusion, spontaneous emission, and removal by the buffer gas, TMB, various photolysis products, and the collision partner of interest. By maintaining cell pressure, TMB partial pressure, and photolysis fluence constant while varying the partial pressure of a particular collision partner, the dependence

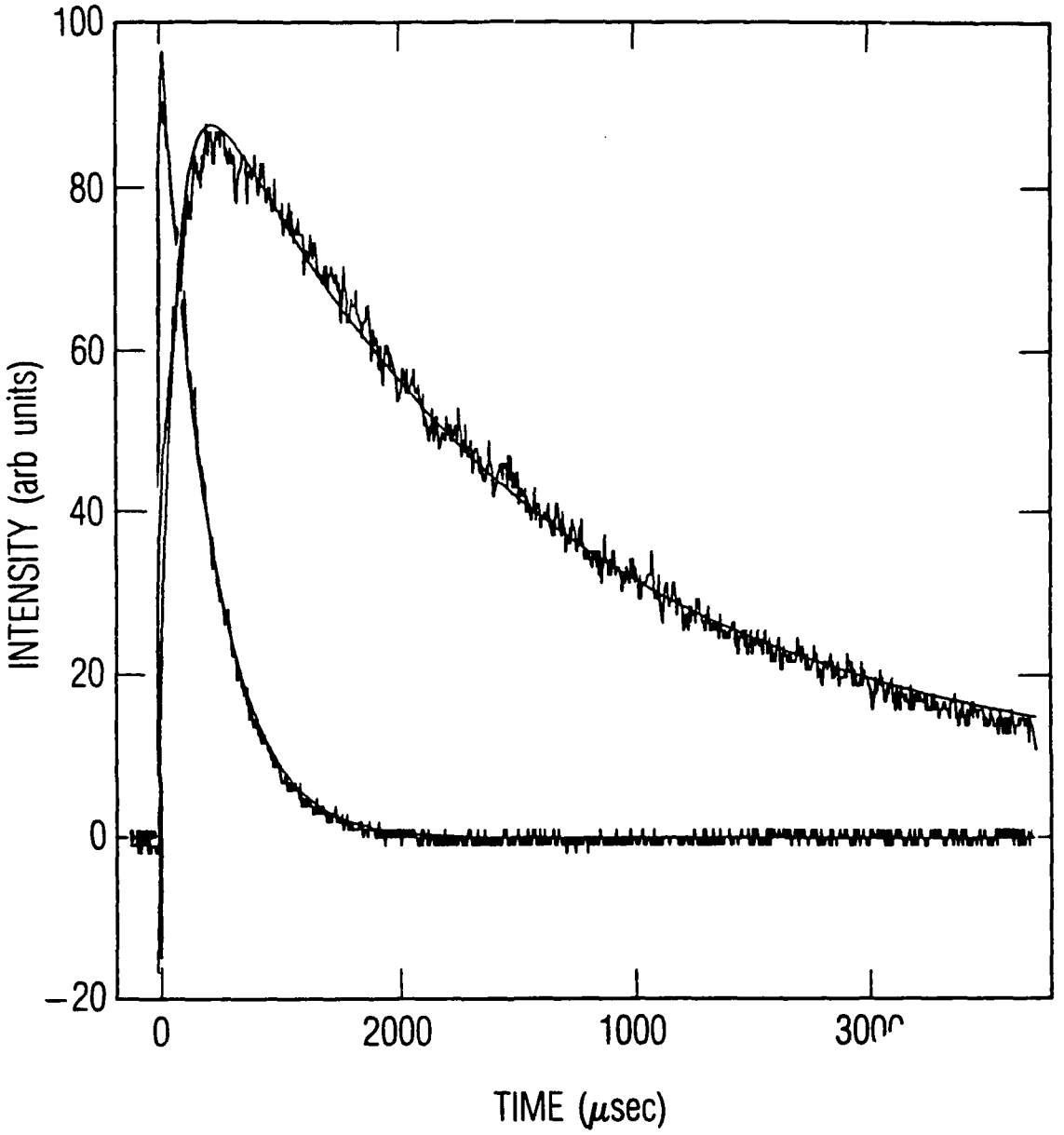

Fig. 2. Representative Bi($^2D_{3/2}$) Emission Traces and Associated Double Exponential Fits. The slower decay was taken with [TMB] = 3.1×10^{12} cm^{-3} in 40 Torr Ar at 295 K. The more rapidly decaying trace was taken with [H_2] = 1.0×10^{18}, [TMB] = 3.1×10^{12} cm^{-3}, balance Ar to 40 Torr. The experimental data are the average of 30 shots.

upon that species can be determined. We obtain removal rate coefficients by plotting the decay rates thus obtained as a function of the number density of the collision partner for a particular set of runs. Figure 3 presents results for quenching by CO_2, H_2, and HF.

Table 1 presents absolute rate coefficients for the removal of $Bi(^2D_{3/2})$ at 295 K by Ar, CO_2, SF_6, H_2, D_2, HD, DF, and TMB. Also given is a lower limit for removal by CH_3. The error quoted is at least 2σ based on the linear least-squares fits of the data. Where appropriate, the results of Bevan and Husain[2] and of Trainor[3] are also provided. Where comparisons are possible, our agreement with Trainor is, in most cases, reasonably good. Although our results for H_2 and D_2 differ from those of Trainor by about a factor of 2, the ratio of the coefficients, k_{H2}/k_{D2}, in both instances is in very good agreement (29.3 vs. 28.8 for Trainor). Trainor has already discussed the discrepancy between his data and that of Bevan and Husain. We would only add that, like Trainor, we have worked at a significantly lower partial pressure of TMB (0.1 vs. 3 mTorr for Bevan and Husain). As a result, because TMB and its CH_3 photofragments are efficient quenchers, our measurements are made against a slower background rate, affording us greater sensitivity to slow processes.

Table 1. Rate Coefficients at 295 K for $Bi(^2D_{3/2})$ + Q → Products
(k: cm^3/molecule-sec)

Quencher	This work	Ref. 3	Ref. 2
Ar	$< 2 \times 10^{-17}$	$< 1 \times 10^{-16}$	
CO_2	$< 8 \times 10^{-17}$	$< 1 \times 10^{-15}$	$< 4 \times 10^{-15}$
SF_6	$< 9 \times 10^{-17}$	$< 6 \times 10^{-16}$	
H_2	$4.1(0.2) \times 10^{-15}$	$7.2(0.3) \times 10^{-15}$	$7.9(0.8) \times 10^{-14}$
D_2	$< 1.4(0.1) \times 10^{-16}$	$< 2.5(1.6) \times 10^{-16}$	$1.1(0.3) \times 10^{-14}$
HF	$2.3(0.2) \times 10^{-14}$		
DF	$< 5.8(0.5) \times 10^{-16}$		
TMB	$7.7(1.4) \times 10^{-11}$	$1.2(0.1) \times 10^{-10}$	
CH_3	$\geq 2.6(0.6) \times 10^{-10}$		

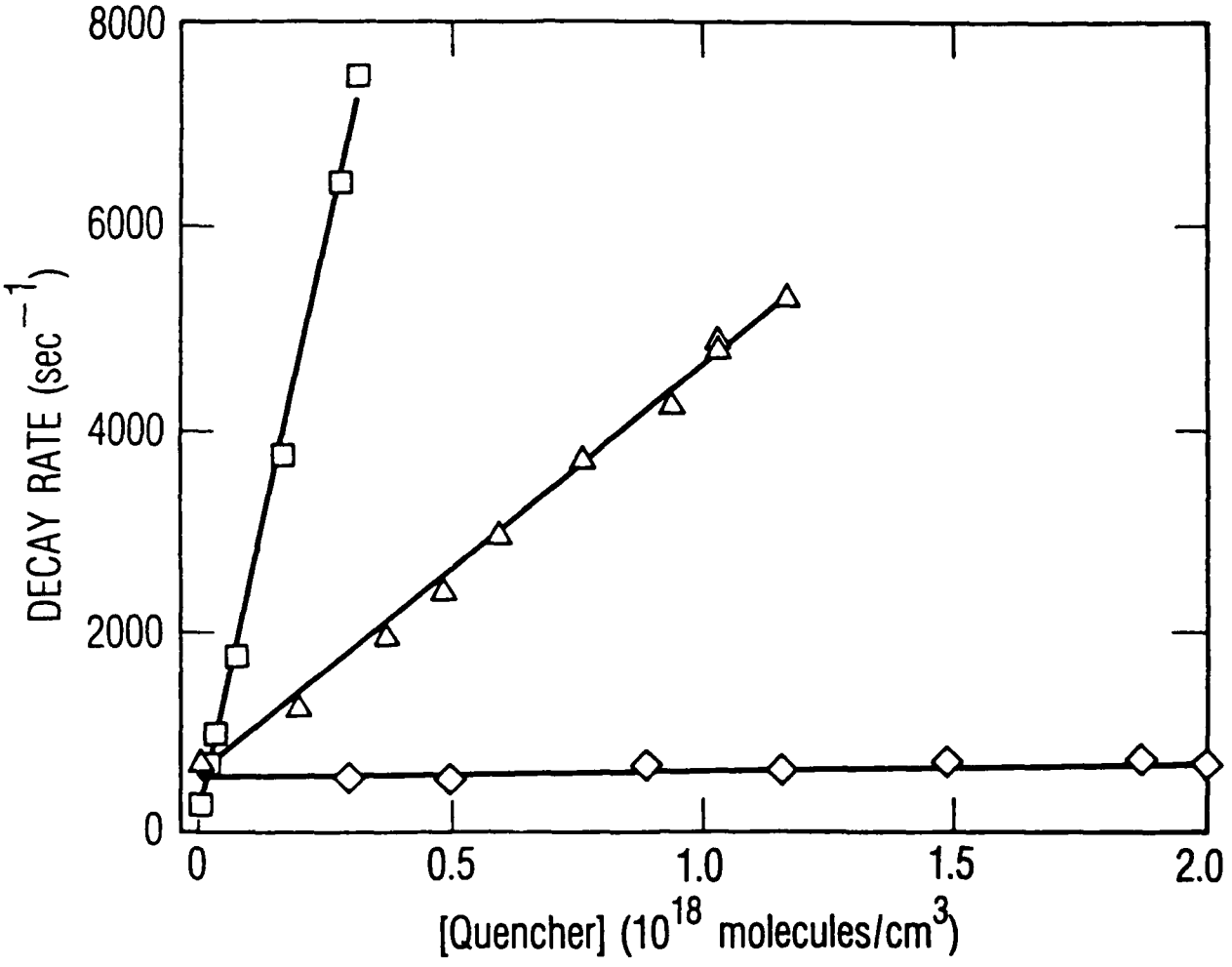

Fig. 3. The Rate of Decay of Bi($^2D_{3/2}$) as a Function of Number Density of the Collison Partner for CO_2 (diamonds), H_2 (triangles), HF (squares), and Linear Least Squares Fits to the Data. The variation in the intercepts is due to the differences in the partial pressure of TMB and laser fluence for a given set of runs.

The enhanced rate of removal of $Bi(^2D_{3/2})$ by H_2 relative to D_2 and by HF relative to DF is worthy of comment. In both cases the protonated form exhibits kinetics which are notably faster than its deuterated analog. Ewing[17] has extended the Sharma-Brau theory[18] of V → V energy transfer to calculate transition probabilities for near resonant E → V transfer in the relaxation of the excited spin-orbit states of Te and Pb by H_2 and D_2, respectively. In this treatment energy transfer is accomplished via a long range attractive potential. For homonuclear diatomics, the coupling is described by a multipole expansion in which the first nonvanishing term is the quadrupole-quadrupole interaction of the initial and final states. In order for us to consider an E → V channel, it is necessary to invoke multiple quanta transitions in the molecular collision partner ($\Delta v = 3$ for H_2, $\Delta v = 4$ for D_2). Direct application of Ewing's model to $Bi(^2D_{3/2})$ predicts a relative mean velocity and J state-averaged rate coefficient of 2.4×10^{-14} cm^3/sec for H_2 and 2.5×10^{-15} cm^3/sec for D_2. These results are a factor of 6 and 20 too large, respectively, compared with our experimentally obtained results for H_2 and D_2. Table 2 provides the parameters that we have used in the calculation and their appropriate references.

It is possible to simplify Ewing's formalism to obtain an estimate of the degree to which long range interactions account for the quenching mechanism. At the same time, by examining the isotopic coefficient ratio, k_{H2}/k_{D2}, much of the uncertainty in the model (principally σ_c, the collision radius at which the model is evaluated) can be reduced in importance.[24] The dominant feature in such a model is the magnitude of the quadrupole moments of the collision partners. By taking the average of the squares of the off diagonal quadrupole matrix elements, $\Delta J = 0, +/-2, 0 +/+ 0$, weighted over 99% of the rotational population for $H_2(\Delta v = 3, J = 0\text{-}3)$ and $D_2(\Delta v = 4, J = 0\text{-}5)$, we obtain a J averaged transition moment and thereby avoid the somewhat arbitrary assignment of a particular rotational level of the collision partner.

Table 2. Parameters Used to Evaluate Long Range Interaction Probability for Near Resonant E → V Transfer

	$Bi(^2D_{3/2})$	+ H_2	+D_2	+ HF	+ DF
Transition (v,J)		0,2 → 3,0	0,0 → 4,2	0 → 3	0 → 4
ΔE (cm^{-1})[a]		-27.3	-39.9	-82.6	-341
A (sec^{-1})[b,c]	$0.21(A_Q)$		$1.17(A_D)$	$0.007(A_D)$	
$Q_{J',J''}^2$ (erg-cm^5)[b,d]	4.7×10^{-51}	5.6×10^{-58}	6.8×10^{-59}		
Q_{av}^2 (erg-cm^5)[d]		2.9×10^{-58}	1.0×10^{-59}		
Radius (Å)[e,f]	1.74	1.48	1.48		
σ_c(Å)		3.22	3.22		

[a]Ref. 19
[b]Ref. 16
[c]Ref. 20
[d]Ref. 21
[e]Ref. 22
[f]Ref. 23

$$Q_{av}^2 = \left(\sum_{J'J''} Q_{J',J''}^2 \times N_J/N_T\right)/n \qquad (5)$$

where $Q_{J',J''}$ is the quadrupole matrix element for a particular J and ΔJ, N_J/N_T is the relative population in a given J and n is the number of transitions over which the sum is taken. The transition probability is proportional to the quotient of the square of the quadrupole moment and the square of the average velocity of the collision pair.

$$P \propto Q^2/v^2 \qquad (6)$$

The rate coefficient, in turn, is the product of the probability and the average velocity of the collision pair.

$$k = Pv \propto Q^2/v \qquad (7)$$

The isotopic ratio, then, is

$$k_{H2}/k_{D2} = Q_{H2}^2 v_{D2}/Q_{D2}^2 v_{H2} \quad (8)$$

Note that we have not explicitly considered the energy defect of the collision. By averaging Q^2 over available J levels, we have implicitly included near resonant collisions. Performing this calculation, we obtain k_{H2}/k_{D2} = 19.9. While this result is smaller than the observed ratio of 29.3, it is in close enough agreement to suggest that the mechanism is a plausible one.

Pritt and Coombe[25] have suggested a long range E → V transfer mechanism for I^* quenching by HF/HCl where the interaction potential may be described in terms of dipole-quadrupole coupling. Their results are normalized by a factor proportional to the product of the squares of dipole transition moment of the molecule and quadrupole transition moment of the atom. Thus

$$k_{nor} = k_{E-V}(A_D \lambda_D^3 A_Q \lambda_Q^5)^{-1} \quad (9)$$

where A_D and λ_D are the spontaneous emission coefficient and wavelength of the molecular dipole vibrational transition of interest and A_Q and λ_Q are the corresponding atomic quadrupole terms. Rotational energy is not considered. Carrying out this procedure for $Bi(^2D_{3/2})$ + HF/DF gives

$$k_{HF,nor} = 2.6 \times 10^{-13} \text{ cm}^3/\text{molec-sec}^3\text{-}\mu\text{m}^8; \ \Delta E = -83 \text{ cm}^{-1}$$

$$k_{DF,nor} = 8.5 \times 10^{-13} \text{ cm}^3/\text{molec-sec}^3\text{-}\mu\text{m}^8; \ \Delta E = -341 \text{ cm}^{-1}$$

Pritt and Coombe compared their normalized values to the results of previous work in which E → V transfer has been established as the dominant relaxation channel for Br^* + HX [5] by means of a Lambert-Salter plot of log k_{nor} vs $-\Delta E$. Our results for $k_{HF,nor}$ are within 25% of the fitted value of the data they present. The value obtained for $k_{DF,nor}$ is about a factor of 5 too large, given the exothermicity of the transfer. Considering the simplicity of the

model, we feel that these results are indicative of the existence of an E → V relaxation channel.

Trainor has quoted a rate coefficient for the removal of $^2D_{3/2}$ by TMB with the caveat that it represents a weighted average of TMB and all photolysis products. We have deduced a rate coefficient for TMB and set a lower limit on the rate coefficient for the CH_3 photofragments.

The rate coefficient for the removal of Bi($^2D_{3/2}$) by the parent TMB was arrived at in the following manner. A range of photolysis fluences was established for which decay rates demonstrated a sensibly linear dependence (< 5 mJ/cm^2). A set of runs with constant TMB was conducted in which fluences were varied within that range. The decay rate for each of these runs was determined and plotted as a function of photolysis power. The y-intercept from the linear least squares fit to this data is the extrapolated rate of removal of the $^2D_{3/2}$ state in the absence of photolysis and therefore in the absence of any photolysis products. This procedure was repeated for a number of partial pressures of TMB. The zero-power intercepts from the resulting plots were, in turn, plotted as a function of their corresponding TMB number density (Fig. 4). The slope of a linear least-squares fit to the data is the rate coefficient for removal by TMB; the intercept should correspond to the inverse radiative lifetime of Bi($^2D_{3/2}$). This is indeed the case; we obtain an intercept of 33.2 sec^{-1} that may be compared to Garstang's calculation[16] for the sum of the Einstein A coefficients for electric quadrapole and magnetic dipole radiation of 31.2 sec^{-1}.

To derive a lower limit on the rate coefficient for CH_3, we make the assumption that the absorption of one 193 nm photon results in the complete decomposition of the parent molecule

$$Bi(CH_3)_3 + n(h\nu) \rightarrow Bi + 3CH_3 \qquad (10)$$

Using the bond energies of Price and Trotman-Dickenson,[26] the three Bi-CH_3 bonds contain a total of 101.4 kcal/mol or about 35,500 cm^{-1}. The Bi($^2D_{3/2}$) state lies 11419 cm^{-1} above the $^4S°$ ground state. It is therefore

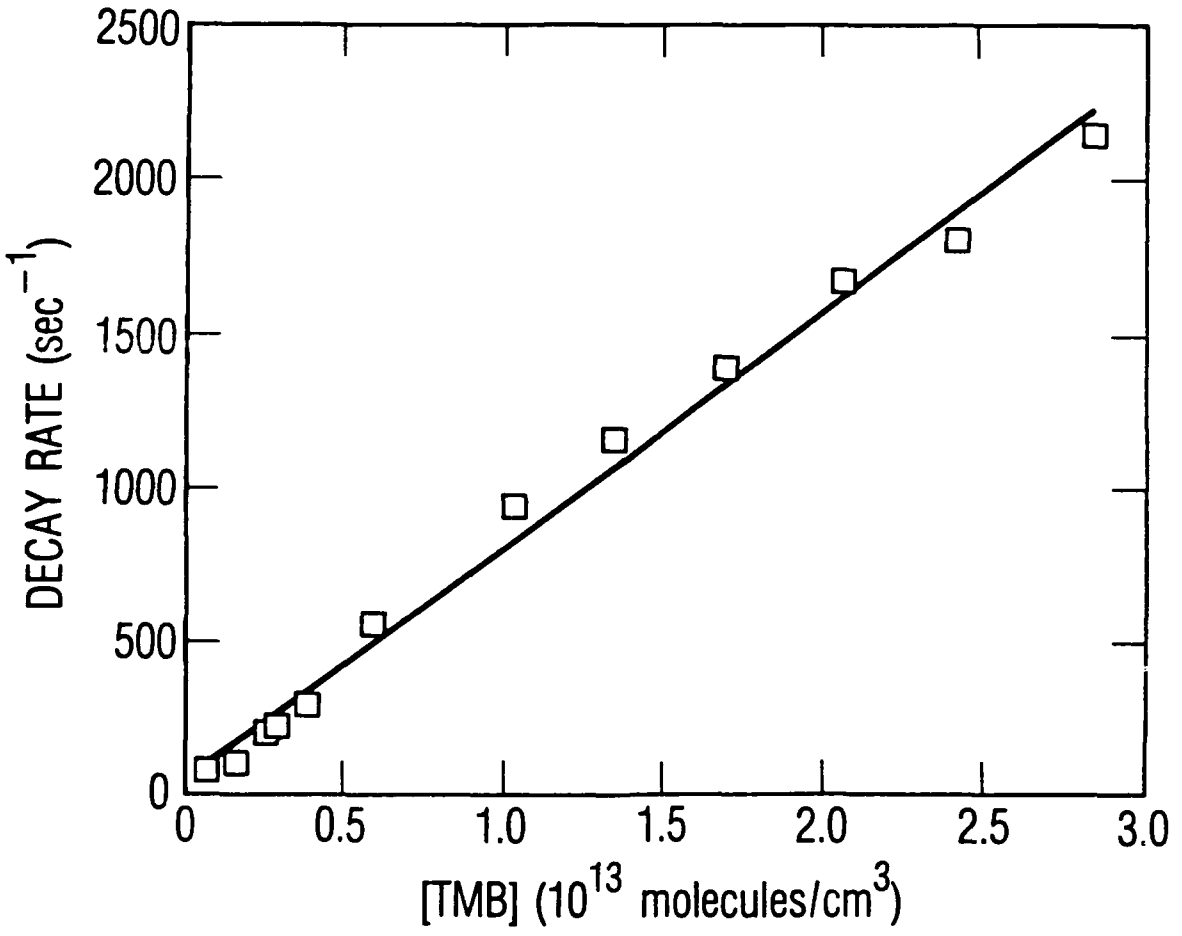

Fig. 4. The Decay Rate of Bi($^2D_{3/2}$) as a Function of TMB Density. The rates were deduced from the y-intercepts of plots of the rate of decay of the $^2D_{3/2}$ state vs laser fluence at a fixed concentration of TMB. This is a true Stern-Volmer plot; the y-intercept is the inverse radiative lifetime of Bi($^2D_{3/2}$).

energetically possible for a single 193 nm photon (51813 cm^{-1}) to provide the requisite energy to cleave the three methyl bonds and populate the $^2D_{3/2}$ level. The following argument is valid, however, as long as Eq. (10) is correct, even if the complete dissociation is a multiple photon process.

The overall rate of decay of the $^2D_{3/2}$ state may be written as

$$R_d = A + k_1[TMB] + k_2[CH_3] \tag{11}$$

where A is the Einstein coefficient for spontaneous emission. According to our assumption

$$[TMB] = [TMB]_0 - [CH_3]/3 \tag{12}$$

$$R_d = A + k_1[TMB]_0 + (k_2 - k_1/3)[CH_3] \tag{13}$$

The fraction of TMB dissociated is

$$[TMB]_{dis}/[TMB]_0 = 1 - \exp(-\sigma I) \tag{14}$$

where σ is the absorption cross section and I is the laser intensity in photons/cm^2 at λ = 193 nm. Therefore,

$$CH_3 = 3[TMB]_0(1 - \exp(-\sigma I)) \tag{15}$$

$$R_d = A + [TMB]_0\{k_1 + (3k_2 - k_1)(1 - \exp(-\sigma I))\} \tag{16}$$

Finally, we can write

$$(R_d - A)/[TMB]_0 = 3k_2 - (3k_2 - k_1)\exp(-\sigma I) \tag{17}$$

This is the case for the data presented in Fig. 5. The plotted rates are obtained from power-dependence measurements at fluences of up to about 55 mJ/cm^2. The accompanying fit is of the form

$$y = A_1 \exp(A_2 x) + A_3$$

This fit gives a rate coefficient for $^2D_{3/2}$ removal by CH_3 (k_2) of 2.6×10^{-10} cm^3/mole-sec. The coefficient for removal by TMB (k_1) is 7.1×10^{-11}, which is in excellent agreement with the value of 7.7×10^{-11} obtained using the zero-power intercept method. Note that our values for TMB and CH_3 bracket Trainor's value of 1.2×10^{-10} for quenching by TMB and photofragments. A value for the absorption cross section of TMB at 193 nm, $\sigma = 3.9 \times 10^{-17}$ cm^2, is also arrived at in the fit. Independent measurements of a purified sample of TMB on an ultraviolet spectrometer at 193 nm yielded a value for σ of 3.8×10^{-17} cm^2. These same absorption measurements gave a value for σ at 211.5 nm of 5.4×10^{-17} cm^2 within 15% of the literature value of 6.3×10^{-17} cm^2.[1] The fact that our model yields values for k_1 and σ which are in good agreement with independent measurements of those same quantities, not only leads us to believe that our value for k_2 is a valid lower limit, but also suggests that the model itself is a plausible representation of at least one of the processes leading to Bi production following photolysis. If so, k_2 may be interpreted as an absolute value.

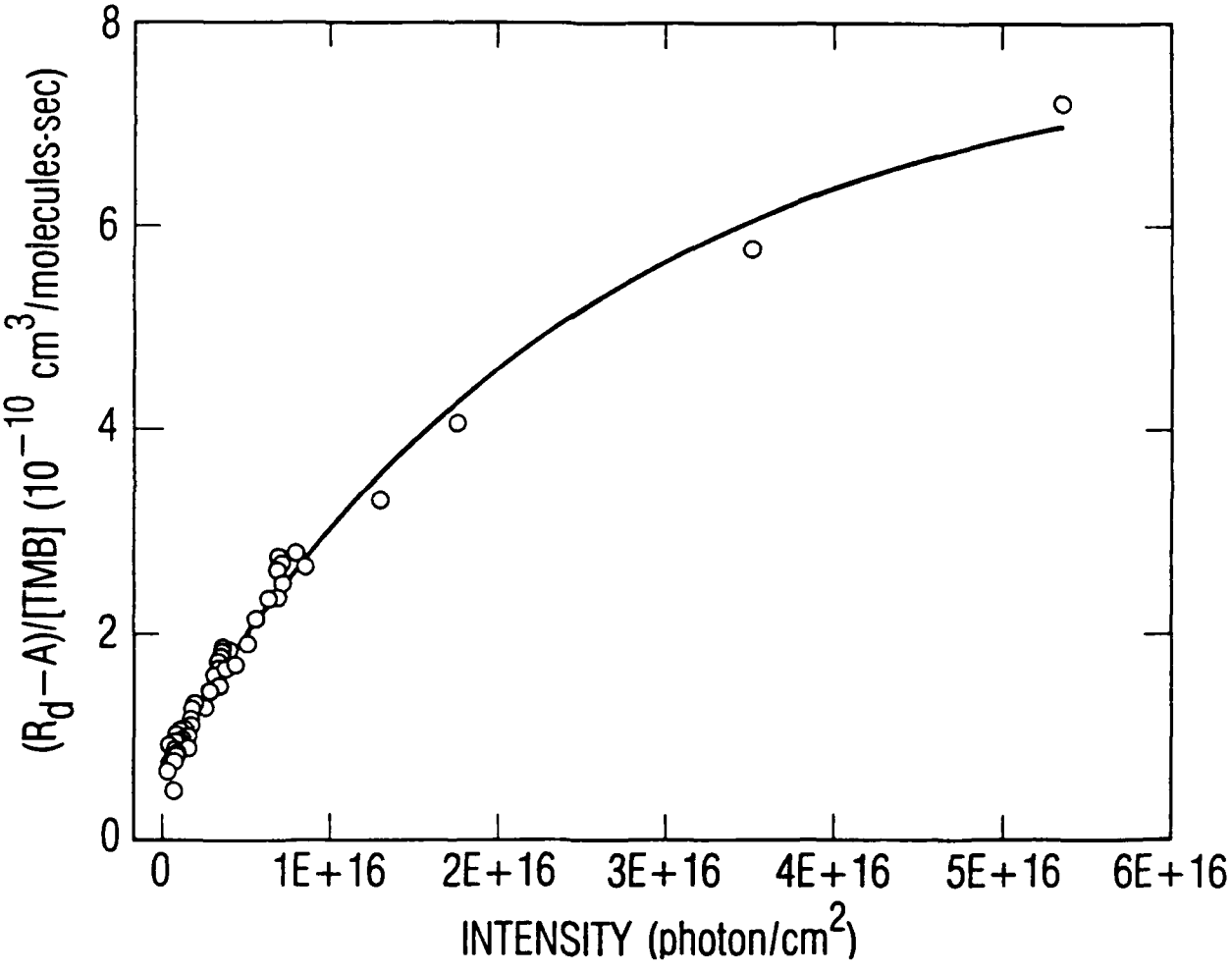

Fig. 5. Experimental Data Corresponding to the Case Described by Eq. (17). Each point represents the total collisional decay rate of Bi($^2D_{3/2}$) for a particular TMB density and photolysis fluence. The fit displayed with the data is a least-squares single exponential in which the baseline is one of the parameters to be determined.

SUMMARY

The rate coefficients for the spin-orbit relaxation of $Bi(^2D_{3/2})$ by a number of nonreactive collision partners have been measured at 295 K. For Ar, CO_2, and SF_6, the rates are slow, $k < 1 \times 10^{-16}$ cm^3/molec-sec. For H_2 and HF, we observe rates that are substantially faster than for their deuterated analogs, D_2 and DF. This isotope effect may be adequately explained in terms of near-resonant, multiquantum E → V transfer via a long range multipole interaction. We have also determined a rate coefficient for quenching by the photolytic precursor, TMB. We present a simple kinetic model which allows us to place a lower limit on the rate of removal by CH_3 photofragments.

REFERENCES

1. J. Connor, P. J. Young, and O. P. Strausz, J. Am. Chem. Soc. 93, 822, (1971).

2. M. J. Bevan and D. Husain, J. Phys. Chem. 80, 217 (1976).

3. D. W. Trainor, J. Chem. Phys. 60, 3094 (1977).

4. D. W. Trainor, J. Chem. Phys. 67 1206 (1977).

5. S. R. Leone and F. J. Wodarczyk, J. Chem. Phys. 60 314 (1974).

6. G. A. Capelle, D. G. Sutton, and J. I. Steinfeld, J. Chem. Phys. 69, 5140 (1978).

7. R. J. Malins and D. W. Setser, J. Phys. Chem. 85, 1342 (1981).

8. J. M. Herbelin, "Efficient Production of Electronically Excited BiF($A0^+$) via Collisions with NF(a)." II, Proceedings of the International Conference on Lasers (1986), pp. 281-288.

9. J. M. Herbelin and R. A. Klingberg, "Short-Wavelength Chemical Lasers based on the Nitrogen Fluoride Molecule," Aerospace Report No. ATR-82(8498)-1 (1 December 1982), pp. 67-70.

10. J. M. Herbelin and R. A. Klingberg, Int. J. Chem. Kinetics 16, 849 (1984).

11. J. B. Koffend, R. F. Heidner III, and C. E. Gardner, J. Chem. Phys. 80, 1861 and references therein (1981).

12. R. F. Heidner III, H. Helvajian, J. S. Holloway, and J. B. Koffend (to be published).

13. D. G. Sutton and S. N. Suchard, Appl. Opt. 14, 1898 (1975).

14. R. J. Donovan, D. Husain, and L. J. Kirsch, Trans. Faraday Soc. 66, 2551 (1970).

15. C. E. Moore, Ed., Atomic Energy Levels, Natl. Bur. Stand. Circ., No. 467 (1958).

16. J. Garstang, Res. Natl. Bur. Stand., Sect A 68, 61 (1964).

17. J. J. Ewing, Chem. Phys. Lett. 29, 50 (1974).

18. R. D. Sharma and C. A. Brau, J. Chem. Phys. 50, 924 (1969).

19. G. Hertzberg, Spectra of Diatomic Molecules, Van Nostrand Reinhold, New York (1950).

20. J. M. Herbelin and G. Emanuel, J. Chem. Phys. 60, 689 (1974).

21. J. D. Poll and L. Wolniewicz, J. Chem. Phys. 68 3053 (1978).

22. J. O. Hirschfelder, C. F. Curtis, and R. B. Bird, Molecular Theory of Gases and Liquids, Wiley, New York, 1110 (1954).

23. C. F. Fischer, Atomic Data 4, 301 (1972).

24. N. P. D. French and K. P. Lawley, Chem. Phys. 22, 105 (1976).

25. A. T. Pritt and R. D. Coombe, J. Chem. Phys. 65, 2096 (1976).

26. S. J. W. Price and A. F. Trotman-Dickenson, Trans. Farad. Soc., 1630 (1958).

LABORATORY OPERATIONS

The Aerospace Corporation functions as an "architect-engineer" for national security projects, specializing in advanced military space systems. Providing research support, the corporation's Laboratory Operations conducts experimental and theoretical investigations that focus on the application of scientific and technical advances to such systems. Vital to the success of these investigations is the technical staff's wide-ranging expertise and its ability to stay current with new developments. This expertise is enhanced by a research program aimed at dealing with the many problems associated with rapidly evolving space systems. Contributing their capabilities to the research effort are these individual laboratories:

Aerophysics Laboratory: Launch vehicle and reentry fluid mechanics, heat transfer and flight dynamics; chemical and electric propulsion, propellant chemistry, chemical dynamics, environmental chemistry, trace detection; spacecraft structural mechanics, contamination, thermal and structural control; high temperature thermomechanics, gas kinetics and radiation; cw and pulsed chemical and excimer laser development including chemical kinetics, spectroscopy, optical resonators, beam control, atmospheric propagation, laser effects and countermeasures.

Chemistry and Physics Laboratory: Atmospheric chemical reactions, atmospheric optics, light scattering, state-specific chemical reactions and radiative signatures of missile plumes, sensor out-of-field-of-view rejection, applied laser spectroscopy, laser chemistry, laser optoelectronics, solar cell physics, battery electrochemistry, space vacuum and radiation effects on materials, lubrication and surface phenomena, thermionic emission, photosensitive materials and detectors, atomic frequency standards, and environmental chemistry.

Computer Science Laboratory: Program verification, program translation, performance-sensitive system design, distributed architectures for spaceborne computers, fault-tolerant computer systems, artificial intelligence, microelectronics applications, communication protocols, and computer security.

Electronics Research Laboratory: Microelectronics, solid-state device physics, compound semiconductors, radiation hardening; electro-optics, quantum electronics, solid-state lasers, optical propagation and communications; microwave semiconductor devices, microwave/millimeter wave measurements, diagnostics and radiometry, microwave/millimeter wave thermionic devices; atomic time and frequency standards; antennas, rf systems, electromagnetic propagation phenomena, space communication systems.

Materials Sciences Laboratory: Development of new materials: metals, alloys, ceramics, polymers and their composites, and new forms of carbon; nondestructive evaluation, component failure analysis and reliability; fracture mechanics and stress corrosion; analysis and evaluation of materials at cryogenic and elevated temperatures as well as in space and enemy-induced environments.

Space Sciences Laboratory: Magnetospheric, auroral and cosmic ray physics, wave-particle interactions, magnetospheric plasma waves; atmospheric and ionospheric physics, density and composition of the upper atmosphere, remote sensing using atmospheric radiation; solar physics, infrared astronomy, infrared signature analysis; effects of solar activity, magnetic storms and nuclear explosions on the earth's atmosphere, ionosphere and magnetosphere; effects of electromagnetic and particulate radiations on space systems; space instrumentation.

...